PROCEEDINGS OF SCIENCE

# Centaurus A as the main source of ultrahigh-energy cosmic rays

**Silvia Mollerach**[ab] **and Esteban Roulet**[ab,*]

[a] *Centro Atómico Bariloche, Comisión Nacional de Energía Atómica*
[b] *Consejo Nacional de Investigaciones Científicas y Técnicas (CONICET)*
*Av. Bustillo 9500, R8402AGP, Bariloche, Argentina*

*E-mail:* eroulet@gmail.com

The possibility that a dominant fraction of the cosmic rays above the ankle is due to the single source Centaurus A is discussed. We focus on the properties of the source spectrum and composition required to reproduce the observations, showing that the nuclei are strongly suppressed for $E > 10Z$ EeV, either by a rigidity-dependent source cutoff or by the photodisintegration interactions with the cosmic microwave background at the giant dipole resonance. The very mild attenuation effects taking place at lower energies imply that the secondary nuclei produced in photodisintegration processes during propagation from this nearby source provide a small contribution. Given the moderate anisotropies observed, the deflections in extragalactic and Galactic magnetic fields should play a crucial role. The diffusion in extragalactic fields as well as the finite source lifetime significantly affect the shape of the observed spectrum. The cosmic-ray flux at tens of EeV is dominated by the CNO component, being actually better reproduced by a mixture of C and O nuclei rather than by just N, while heavier nuclei become dominant above 70 EeV. The cosmic ray flux at a few EeV should mostly result from a more isotropic light component associated with a population of extragalactic sources. The inclusion of the subdominant contribution of heavy nuclei from the Galactic component helps to reproduce the observations around 1 EeV.

39th International Cosmic Ray Conference (ICRC2025)
15 – 24 July, 2025
Geneva, Switzerland


*Speaker





PoS(ICRC2025)372

## 1. Introduction

The origin of ultrahigh-energy cosmic rays (UHECRs) is one of the important open problems in astrophysics. The clues we have to decipher it come from the measured cosmic-ray (CR) spectrum, their inferred composition, and the anisotropies in their arrival directions. However, the observed quantities at Earth are related to the source properties in a very non-trivial way, given that the CR fluxes can be reshaped during their propagation through the intergalactic radiation backgrounds and intervening magnetic fields, the nuclei can be photodisintegrated on the way, and the CR trajectories may be strongly deflected.

Two very important features of the spectrum are the ankle at about 5 EeV and the strong suppression taking place above about 50 EeV [1, 2]. The first feature involves a hardening of the spectrum, which is usually interpreted as a consequence of the emergence of a new contribution to the CR fluxes on top of the steeply falling spectrum present at lower energies. The suppression at the highest energies may be due either to a cutoff in the acceleration at the sources or to the attenuation effects during propagation, or to both effects combined. The composition, as inferred from the observed maximum depth of the air-shower development [3], is found to become heavier for increasing energies. In particular, the values of $\langle \ln A \rangle$ (with $A$ being the mass number) typically correspond to light elements being present near the ankle, with CNO group elements becoming then dominant up to the suppression energy and even heavier elements contributing at the highest energies [4]. The dispersion of the masses, which can be quantified by the variance $\mathrm{Var}(\ln A)$, becomes small above the ankle energy, being consistent with a very small overlap between different CR masses at those energies. The main anisotropy observed is the dipolar distribution determined above 8 EeV, of amplitude 7.4% and pointing $\sim 115^\circ$ away from the Galactic center, which grows to 17% above 32 EeV [5]. Also hints of localized excesses on intermediate angular scales (of about $30^\circ$ radius) appear for energies larger than about 40 EeV in a region towards the direction of Centaurus A, in which the observed flux is about 40% higher than the isotropic expectation [6, 7]. Other anisotropies, also on intermediate angular scales and appearing in different regions of the sky, have been reported by the Telescope Array Collaboration [8], although they have not been confirmed in the searches performed with the Auger Observatory [9].

## 2. The Centaurus A scenario

In this presentation, we want to discuss the scenario put forward in [10], in which most of the CRs with energies above the ankle one come from the radiogalaxy Centaurus A (whose optical counterpart is the galaxy NGC 5128). Cen A is the closest radiogalaxy, at just 3.8 Mpc from us, and it features powerful outflows in different stages of evolution [11]. These include giant radio lobes extending for about 0.5 Mpc, a middle northern lobe extending 40 kpc, inner jets of few kpc and pc scale jets in the nuclear region. The AGN activity associated with the central supermassive black hole (of mass $5.5 \times 10^7\, M_\odot$), was likely enhanced as the result of a galaxy merger that took place about 2 Gyr ago, with the middle lobe having an age of few hundred million years and the inner jets being younger. All these features make Cen A a particularly attractive candidate UHECR source, in which the jet activity could be responsible for the acceleration (or for the reacceleration of CRs previously accelerated to lower energies inside the galaxy) up to ultrahigh energies.

Being this galaxy so close, one expects that the CR attenuation during propagation should not be strong, with the main relevant process eventually being the photodisintegration of the nuclei upon interactions with the CMB, which due to the giant dipole resonance reaches its maximum strength for CR energies $E \simeq 10A$ EeV. For CRs with that energy, a total disintegration could occur just after traveling about 4 Mpc. However, in the scenario discussed, the CR rigidities are found to satisfy $E/Z < 10$ EeV, and hence $E/A \simeq 0.5E/Z$ is in general below the threshold of the giant resonance. Interactions with the more energetic extragalactic background light have much larger associated interaction lengths, as also happens for the interactions of the protons at these rigidities. All this implies that, in the Cen A source scenario, the cutoff in the source acceleration will play the dominant role in explaining the high-energy spectral suppression. On the other hand, when a distribution of sources is instead considered, the attenuation due to interactions plays a more important role in shaping the suppression, with the source cutoff being mostly constrained by the copious production through these interactions of H and He secondaries, which show up around the ankle energy.

The baseline scenario considers that five representative elements (H, He, N, Si and Fe) are emitted from the source with a power-law spectrum having a rigidity-dependent cutoff. To account for the measurements below the ankle energy, an additional population of sources, probably originating from a large number of less powerful sources distributed over space, is required. The sources in this population need to have a steeper CR spectrum and to emit relatively lighter elements. We have also found that to better reproduce the features in the spectrum and composition, it is convenient to consider that the nearby source (Cen A) emits, instead of N, a combination of C and O nuclei, which are actually the most abundant elements in the CNO group. Given that the C and O masses differ by about 25%, this can lead to features in the spectrum near the suppression energy that are noticeable. In contrast, the spectrum at Earth resulting from a population of sources distributed over redshift (which is the main alternative model for the high-energy population) would lead, because of the averaging effects from sources at different distances, to similar spectral shapes for the assumption that only N or instead a mixture of C and O describe the CNO group. Let us note that a possible source type that could naturally inject a dominant fraction of C and O, with little H, would be the tidal disruption of white dwarfs by intermediate mass black holes ($10^3$ to $10^5\, M_\odot$) [12, 13]. We also found that including the tail of the Galactic CR contribution, consisting mostly of heavy Si and Fe group elements [14], helps to account for the observed dispersion in the CR masses at the lowest energies considered ($\sim$ 1 EeV).

Given that the CR anisotropies observed above the ankle are moderate, a scenario with just one nearby source (Cen A) will not be realistic unless there are significant CR deflections caused by magnetic fields. Our galaxy is known to have both coherent and random magnetic fields, with a typical strength of a few $\mu$G. Their precise structure is not well known, but several models exist to describe them. Regarding the extragalactic magnetic field (EGMF) [15, 16], its properties are even more uncertain and it is expected to have a different strength inside the voids ($B_{\rm rms} < 1$ nG) than in the sheets and filaments ($10 < B_{\rm rms}/{\rm nG} < 100$) of the large-scale structure. These latter values are hence those expected to be present within the Local Supercluster in which we are located, whereas inside the galaxy clusters the magnetic fields are observed to have strengths of a few $\mu$G.

We will model the EGMF as a uniform turbulent field with root mean square strength $B_{\rm rms}$, coherence length $l_{\rm coh}$, and consider that it has a Kolmogorov spectrum of turbulence. This will

describe the field within our local neighborhood, encompassing in particular the Cen A galaxy, so that a typical strength of several tens of nG could be expected. One also expects that $10\,\mathrm{kpc} < l_{\rm coh} < 1\,\mathrm{Mpc}$, i.e. that $l_{\rm coh}$ lies between galactic scales and typical intergalactic distances.

A particle of charge $eZ$ traveling through a magnetic field $B$ has an associated Larmor radius

$$r_{\rm L} \equiv \frac{E}{eZB} \simeq 1.1 \frac{E/\mathrm{EeV}}{ZB/\mathrm{nG}}\,\mathrm{Mpc} \tag{1}$$

and, since above the ankle energy the typical CR rigidities are $E/Z \simeq$ few EeV, the presence of magnetic fields with tens of nG strength is expected to have sizable effects on CRs from the Cen A source lying at a distance $r_{\rm s} \simeq 4\,\mathrm{Mpc}$.

Let us then first consider the possible implications of the presence of the turbulent EGMF [17–19]. In this case, the typical deflections in the quasi-rectilinear regime and after traveling several coherence lengths are

$$\theta_{\rm rms} \simeq 28^\circ \frac{10\,\mathrm{EeV}}{E/Z} \frac{B_{\rm rms}}{20\,\mathrm{nG}} \sqrt{\frac{l_{\rm coh}}{100\,\mathrm{kpc}} \frac{r_{\rm s}}{4\,\mathrm{Mpc}}}, \tag{2}$$

with $\theta$ measured with respect to the source direction. More generally, for cosmic rays diffusing from a steady source

$$\langle \cos\theta \rangle \simeq \frac{1 - \exp\left(-3R - 3.5R^2\right)}{3R}, \tag{3}$$

with $R \equiv r_{\rm s}/l_D$, and the diffusion length

$$l_D \simeq l_{\rm coh} \left[4(E/E_{\rm c})^2 + 0.9E/E_{\rm c} + 0.23(E/E_{\rm c})^{1/3}\right] \tag{4}$$

is the distance after which the typical deflection is 1 rad. Here, the critical energy $E_{\rm c}$ is that for which $r_{\rm L}(E_{\rm c}) = l_{\rm coh}$, so that $E_{\rm c} \simeq 0.9\,Z(B_{\rm rms}/\mathrm{nG})(l_{\rm coh}/\mathrm{Mpc})\,\mathrm{EeV}$.

The diffusion process actually also affects the CR density around the source because the CRs take more time to escape from the source region and hence their density gets enhanced with respect to the value obtained in the case of rectilinear propagation. For a steady source, this enhancement amounts to a factor $1/\langle\cos\theta\rangle$, reflecting the overall conservation of the flux through any spherical surface around the source [20]. Note that if the nearby source dominates the flux above the ankle and it is responsible for the observed dipole, which has a typical amplitude $d = 3\langle\cos\theta\rangle \simeq 0.1$, one expects that the diffusive flux enhancement should be about a factor 30 at $E \simeq 10\,\mathrm{EeV}$. In the case of a non-steady source, as would be the case for Cen A for which one expects it to have been active for about $10^8$ to $10^9$ yr, other effects also become relevant. In particular, a suppression of the flux will occur at low energies when the typical propagation time from the source up to us becomes larger than the source age. This is called the magnetic horizon effect.

The enhancement factor is plotted in Fig. 1 as a function of $E/R_{\rm c}$, with $R_{\rm c} \equiv E_{\rm c}/Z$, for different nuclear species and for different coherence lengths, considering that the source started to emit steadily since a time $t_i = 50 r_{\rm s}/c$ before the present time. Note that the maximum enhancement in this case occurs for an energy $E \simeq 0.3ZR_{\rm c}$, and therefore, for this peak to be above the ankle for N nuclei (which is desirable to reproduce the observations), one needs $R_{\rm c} \simeq 3\,\mathrm{EeV}$. Given that

$$B_{\rm rms} \simeq 33 \frac{R_{\rm c}}{3\,\mathrm{EeV}} \frac{100\,\mathrm{kpc}}{l_{\rm coh}}\,\mathrm{nG}, \tag{5}$$

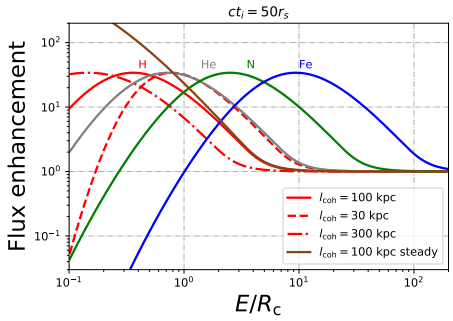


**Figure 1:** Flux enhancement factor as a function of $E/R_c$ considering that $ct_i = 50r_s$. Results are shown for different nuclei with $l_{coh} = 100$ kpc and for different values of $l_{coh}$ in the case of H nuclei.

this points towards magnetic field values $B_{rms} \simeq 30\,\mathrm{nG}(100\,\mathrm{kpc}/l_{coh})$ for this scenario to work. On the other hand, the maximum density enhancement achieved is about $0.8ct_i/r_s$, and in order that the dipole be at the level $d < 0.1$ one needs that $ct_i > 30r_s$. The density enhancement also reduces the energy requirements at the source, and to reproduce the observed local UHECR density a UHECR luminosity $\mathcal{L}(E > 10\,\mathrm{EeV}) \simeq 10^{41}$ erg/s would be necessary. This is more than two orders of magnitude smaller than the power of the Cen A jet at present.

It is important to realize that when the propagation is diffusive and the density enhancement sizable, the angular distribution of the CRs arriving at Earth is not just a Gaussian (or Fisher) distribution around the source direction, but there is also an isotropic component arising from the CRs that performed several turns before reaching the Earth (thus traveling distances $ct \gg r_s$). One indeed has that [21]

$$\frac{1}{N}\frac{\mathrm{d}N}{\mathrm{d}\cos\theta} \simeq \frac{i}{2} + (1-i)\frac{\kappa\exp(\kappa\cos\theta)}{2\sinh\kappa}, \tag{6}$$

where the concentration parameter $\kappa$ and the isotropic fraction $i$ can be expressed in terms of $\langle\cos\theta\rangle$ and $\langle\cos^2\theta\rangle$. In the previous expression, the contribution concentrated around the source direction

model G-NE-4Mpc(CO), $ct_i = 50r_s$, EGMF with $l_{coh} = 100$ kpc

| $\Delta$ | $\gamma_s$ | $R^s_{cut}$ [EeV] | $f^s_H$ | $f^s_{He}$ | $f^s_C$ [%] | $f^s_O$ | $f^s_{Si}$ | $f^s_{Fe}$ | $\gamma_L$ | $R^L_{cut}$ [EeV] | $f^L_H$ | $f^L_{He}$ [%] | $f^L_N$ | $R_c$ [EeV] | $\frac{\chi^2}{dof}$ |
|---|---|---|---|---|---|---|---|---|---|---|---|---|---|---|---|
| 2 | 0.4 | 6.0 | 0 | 86 | 12 | 2.1 | 0.3 | 0 | 3.0 | 8.2 | 13 | 83 | 0 | 1.4 | 2.90 |
| | 1.7 | 24 | 9.5 | 39 | 31 | 18 | 2.6 | 0.1 | 3.0 | 8.4 | 21 | 65 | 14 | 3.6 | 3.07 |
| 1 | 1.2 | 7.9 | 0 | 65 | 21 | 13 | 0.8 | 0.1 | 2.9 | 7.6 | 13 | 83 | 0 | 2.8 | 3.05 |
| idem with $E \times 1.14$ | | | | | | | | | | | | | | | |
| 2 | 1.9 | 29 | 27 | 17 | 32 | 20 | 3.1 | 1.1 | 3.0 | 10 | 17 | 63 | 20 | 4.7 | 1.98 |
| | 1.2 | 8.8 | 0 | 66 | 25 | 6.9 | 1.6 | 0.1 | 2.9 | 10.2 | 5.8 | 90 | 0 | 3.8 | 2.38 |
| 1 | 2.0 | 23 | 27 | 13 | 32 | 23 | 2.9 | 1.5 | 3.0 | 11 | 16 | 64 | 19 | 4.8 | 2.18 |

**Table 1:** Parameters of the fit to the flux and composition for the different scenarios including an EGMF with $l_{coh} = 100$ kpc and a source emitting steadily since an initial time $t_i = 50r_s/c$, also considering emission of C and O from the nearby source rather than N. Results are shown for $\Delta = 2$ and 1, and also when rescaling the observed energies by a factor 1.14. The index 's' corresponds to the Cen A source while 'L' to the low-energy population.

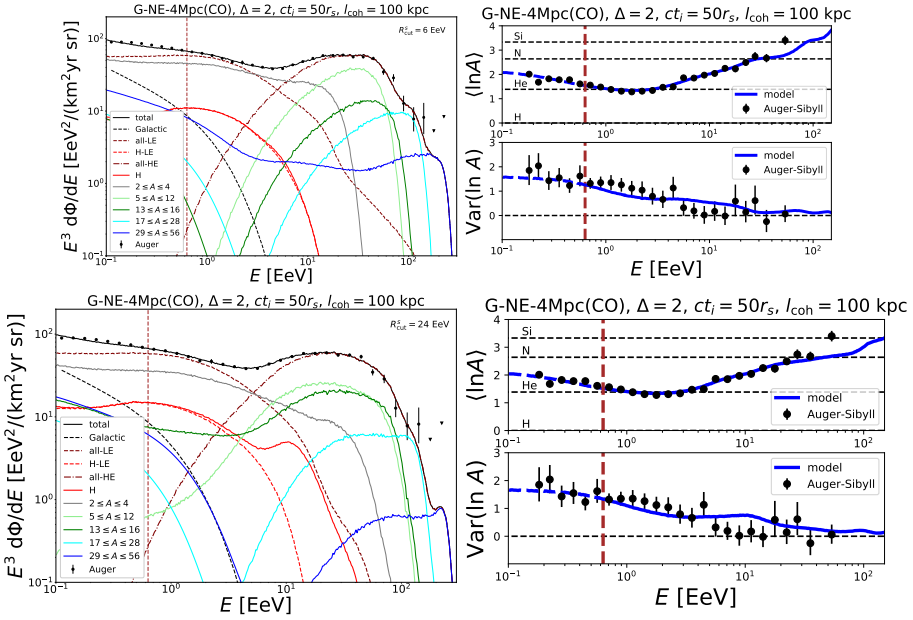


**Figure 2:** Spectrum and composition in the scenarios including the effects of EGMF with $l_{\rm coh} = 100$ kpc and a source emitting steadily since an initial time $t_i = 50 r_{\rm s}/c$. Results for two different values of the source cutoff are shown. The case with $\Delta = 2$ and for Sibyll 2.3c is shown. Vertical dashed lines indicate the threshold of the fit ($10^{17.8}$ eV). We considered C and O rather than N for the HE population and included the Galactic component.

involves CRs emitted relatively recently, at times $t <$ few $r_{\rm s}/c$, while those emitted earlier contribute mainly to the isotropic part.

The results of the fit to the spectrum and composition data from the Auger Observatory [1, 3], which largely dominate the UHECR statistics at present, are reported in Table 1, where the parameter $\Delta$ characterizes the steepness of the source cutoff, which is assumed to scale as $\mathrm{sech}((E/ZR_{\rm cut})^{\Delta})$. We considered values of $\Delta = 1$ or 2, $ct_i = 50 r_{\rm s}$ and $l_{\rm coh} = 100$ kpc. They are illustrated in Fig. 2, for the case $\Delta = 2$, where we show two different fitted scenarios having cutoff rigidities at the source of $R^{\rm s}_{\rm cut} = 6$ EeV and 24 EeV respectively. Note that near the instep spectral feature at around 15 EeV, different amounts of He are present in the two scenarios. Also a broader C and O contribution and some H are present for the larger cutoff value, for which the interactions during propagation are actually not completely negligible (see, for instance, the pile-up in the Fe component appearing at the highest energies).

To study the arrival direction distribution, it is necessary to also include the effects of the Galactic magnetic field deflections, which can lead to lensing effects involving multiple imaging, and (de)magnification of the fluxes [22–24]. We just consider the Galactic field regular component, from [25], given that in our scenario the effects of the Galactic random fields are expected to be subdominant with respect to the EGMF ones discussed previously. The relative fluxes as a function of the arrival directions, in Galactic coordinates, are displayed for different energies in Fig. 3, in which we considered the results obtained after scaling the measured energies up by 14% (which is the experimental systematic uncertainty) given that this improves the goodness of the fit to the spectrum and composition (see the Table). One can appreciate that the distributions are in a

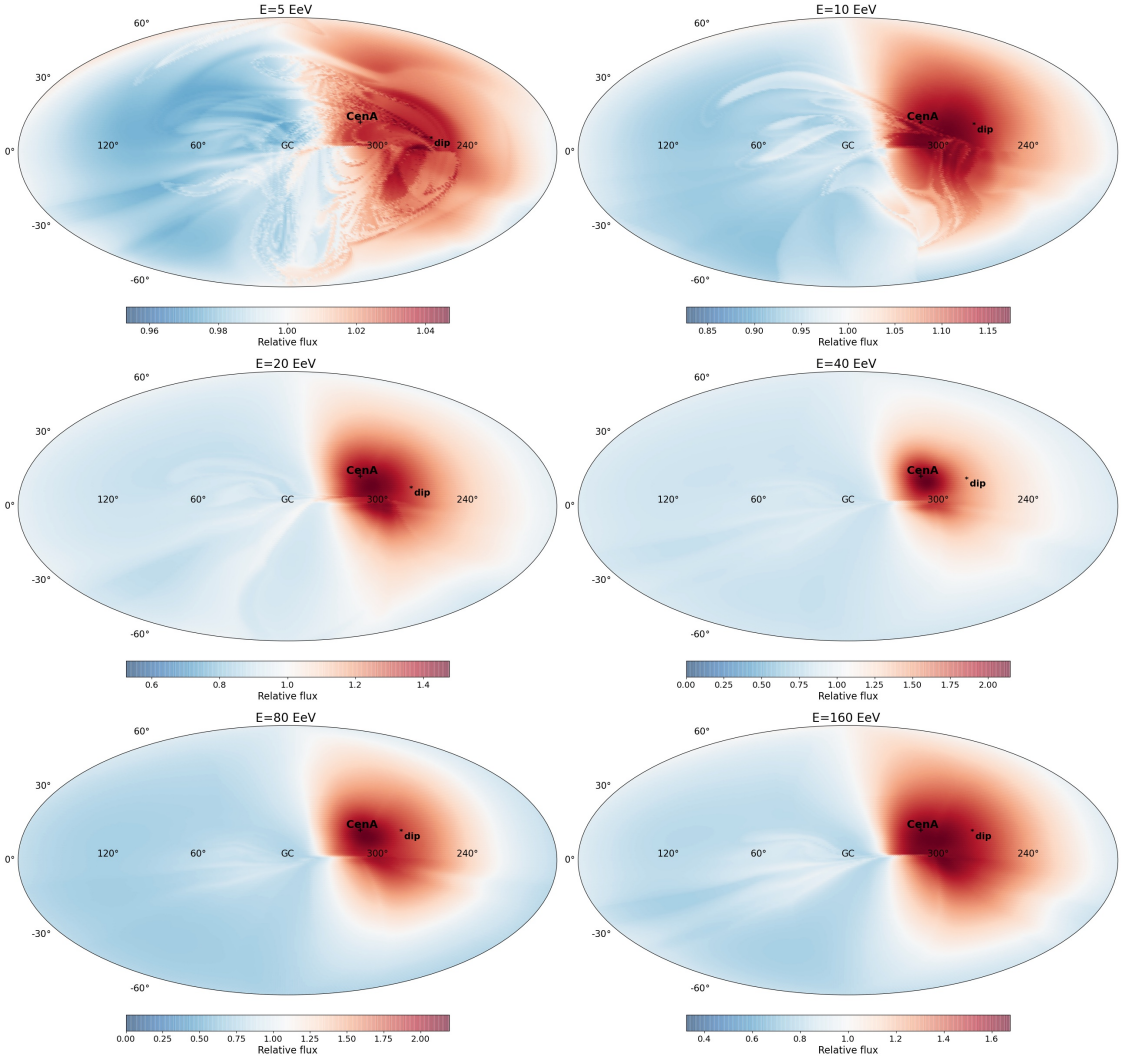


**Figure 3:** CR flux, normalized to the average flux in the whole sky, as a function of galactic coordinates for the model with $\Delta = 2$, $ct_i = 50 r_s$ and $l_{coh} = 100$ kpc (considering the observed energies scaled by 1.14). Different panels correspond to different energies, as indicated, and the label 'dip' indicates the direction of the resulting dipole. The location of Cen A is also indicated.

general qualitative agreement with the features observed. They show a mostly dipolar distribution at $E < 20$ EeV, whose amplitude grows with energy and points in a direction (indicated as 'dip' in the maps) slightly displaced with respect to Cen A towards the outer spiral arm direction. At higher energies, more localized excesses appear close to the Cen A direction and on angular scales of a few tens of degrees. It is interesting that the anisotropies are more pronounced at 40 to 80 EeV, where the flux is dominated by CNO elements that reach the highest rigidity values (5 to 10 EeV), while at higher energies there is a larger contribution from Si and Fe nuclei that actually have a lower average rigidity. The effects of the sizable EGMF deflections could also help to understand why most of the highest energy events have no obvious nearby source candidate. Let us mention that the study of the He contribution at energies of 10 to 20 EeV could also be important to distinguish

between the possible scenarios.

## References


[1] P. Abreu et al. (Pierre Auger Collaboration), Eur. Phys. J. C 81 (2021) 966

[2] V. Verzi, D. Ivanov and Y. Tsunesada, Prog. of Th. and Exp. Phys. 12 (2017) 12A103

[3] A. Yushkov for the Pierre Auger Collaboration, PoS(ICRC2019)482

[4] A. Abdul Halim et al. (Pierre Auger Collaboration), JCAP 05 (2023) 024

[5] A. Aab et al. (Pierre Auger Collaboration), Astrophys. J. 868 (2018) 4

[6] A. Aab et al. (Pierre Auger Collaboration), Astrophys. J 804 (2015) 15

[7] G. Golup for the Pierre Auger Collaboration, PoS(ICRC2023)252

[8] R.U. Abbasi et al. (Telescope Array Collaboration), Astrophys. J. 862 (2018) 91

[9] A. Abdul Halim et al. (Pierre Auger Collaboration), Astrophys. J 984 (2925) 123

[10] S. Mollerach and E. Roulet, Phys. Rev. D 110 (2024) 063030

[11] F.P. Israel, Astron. Astrophys. Rev. 8 (1998) 237

[12] B.T. Zhang, K. Murase, F. Oikonomou and Z. Li, Phys. Rev. D 96 (2017) 063007

[13] R.A. Batista and J. Silk, Phys. Rev. D 96 (2017) 103003

[14] S. Mollerach and E. Roulet, JCAP 03 (2019) 017

[15] J.P. Vallée, New Astronomy Reviews 55 (2011) 91

[16] E. Carretti and F. Vazza, Universe 2025, 11(5), 164

[17] D. Harari, S. Mollerach, E. Roulet and F. Sánchez, JHEP 03 (2002) 045

[18] D. Harari, S. Mollerach and E. Roulet, Phys. Rev. D 89 (2014) 123001

[19] D. Harari, S. Mollerach and E. Roulet, Phys. Rev. D 93 (2016) 063002

[20] S. Mollerach and E. Roulet, Phys. Rev. D 99 (2019) 103010

[21] D. Harari, S. Mollerach and E. Roulet, Phys. Rev. D 103 (2021) 023012

[22] S. Mollerach and E. Roulet, Phys. Rev. D 105 (2022) 063001

[23] D. Harari, S. Mollerach and E. Roulet, JHEP 08 (1999) 022

[24] D. Harari, S. Mollerach and E. Roulet, JHEP 02 (2000) 035

[25] R. Jansson and G.R. Farrar, Astrophys. J. 757 (2012) 14